

An analytical and experimental study was made of a heat pipe with the capillary structure of the evaporator comprising an array of closed channels. Here the results are reported.

An analysis of the results of studies pertaining to heat transfer during boiling of a liquid in capillary channels under forced circulation [1, 2] indicates that the heat-transfer coefficient from channel wall to boiling liquid is one order of magnitude higher than permissible in heat pipes with reticular wicks. Accordingly, the capillary structure of the evaporator segment in recently proposed heat pipes [3] comprises an array of closed parallel channels (Fig. 1). Such a capillary structure can be produced by insertion into the cylindrical housing 1 of a hollow sleeve 2 with a series of circumferential grooves 3 on the outside surface, grooves whose profile can be of any shape and thus also of standard shape. The working liquid is fed to these circumferential grooves through axial channels 4 and the vapor is removed from them through radial channels 5. It is feasible, in principle, to build such heat pipes with a rectangular or any other cross section.

As the hydrodynamic limit on heat transfer (by a heat pipe) is regarded the thermal flux level at which: 1) the mass fraction of vapor in the stream leaving the circumferential grooves of the evaporator is equal to unity; 2) the length of the economizer segment is negligible as compared with that of the evaporation segment on film surface; 3) the film of liquid is retained throughout a cycle of vapor slug nucleation and expansion; and 4) break-away of a new liquid plug occurs only after the preceding one has moved out completely.

Assuming that the liquid enters a circumferential channel at the saturation temperature (Fig. 2) and disregarding the heat of superheating along the economizer segment, we can write

$$Q = G_0 r. \quad (1)$$

The quantity  $G_0$  will be determined from the equation of pressure balance

$$\Delta P = \Delta P_1 + \Delta P_2 \pm \Delta P_3, \quad (2)$$

where  $\Delta P$  is the driving pressure head;  $\Delta P_1$ , hydraulic losses in the closed circumferential capillary channels of the evaporator;  $\Delta P_2$ , hydraulic losses associated with liquid and vapor in axial and radial channels of the evaporator, along the transport segment, and in the condenser; and  $\Delta P_3$ , gravitational component of the head, viz., the difference in elevation between evaporator and condenser.

Circulation of the working liquid through the heat pipe is produced by the capillary head and, accordingly,  $\Delta P$  can be determined from the Laplace equation

$$\Delta P = \sigma \left( \frac{1}{R_{\min}} + \frac{1}{R_{\max}} \right), \quad (3)$$

where  $R_{\min}$  and  $R_{\max}$  are the principal radii of curvature of the interphase boundary in the evaporator, i.e., of the meniscus of the liquid plug.

For evaluating the hydraulic losses  $\Delta P_1$  in the closed circumferential capillary channels, we use the model of quasisteady homogeneous flow [4]. Here

$$\Delta P_1 = \Delta P_f + \Delta P_i, \quad (4)$$

where  $\Delta P_f$  are the frictional losses and  $\Delta P_i$  are the inertial losses.

The frictional losses  $\Delta P_f$  during adiabatic flow of a plug appear as three component pres-

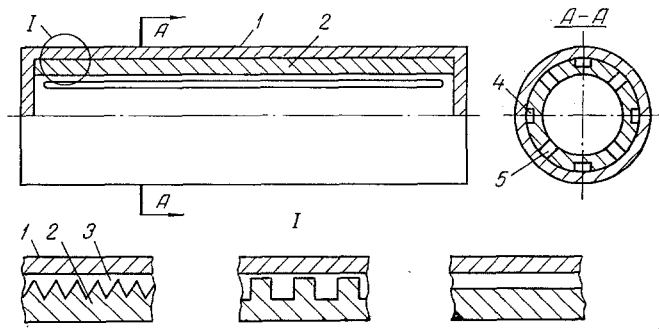


Fig. 1. Design of a heat pipe with a closed capillary structure.

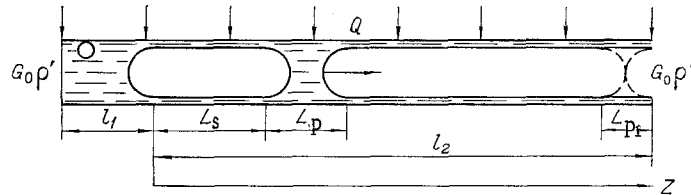


Fig. 2. Geometrical model for calculation of the limiting heat load on a capillary:  $l_1$ ) economizer segment and  $l_2$ ) evaporator segment along the microfilm surface.

sure drops: I) in the liquid plug; II) at the ends of the bubble; and III) along the bubble. The interphase boundary in capillary channels has an almost uniform curvature and, therefore, the last two component pressure drops are nearly zero. The mean pressure gradient along a channel is

$$\frac{dP}{dZ} = \frac{1}{2} \lambda \frac{\rho'}{d_h} J^2 \left( \frac{L_p}{L_p + L_s} \right), \quad (5)$$

where

$$\lambda = f(N_{ReJ}); J = \frac{G'}{\rho' F} + \frac{G''}{\rho'' F}.$$

Since our system is a nonadiabatic one so that the referred velocity and the attendant friction coefficient vary appreciably, and the liquid plug becomes shorter while the vapor slug becomes longer, functional relations for these quantities must be introduced into expression (5) for calculating the frictional losses. When the capillary is uniformly heated, then the referred velocity as well as the length of the liquid plug and the length of the vapor slug vary linearly

$$J(z) = J_0 - (J_0 - J_1) \frac{Z}{l}, \quad (6)$$

where

$$J_0 = \frac{G_0}{\rho' F}; J_1 = \frac{G_0}{F} \left( \frac{x}{\rho''} + \frac{1-x}{\rho'} \right).$$

Inasmuch as  $J_0 \ll J_1$ , we have

$$J(z) = J_1 \frac{Z}{l}. \quad (7)$$

The length of the liquid plug is correspondingly determined as

$$L_{p(z)} = L_{p0} - (L_{p0} - L_{p1}) \frac{Z}{l}, \quad (8)$$

where  $L_{p0}$  and  $L_{p1}$  denote the length of the liquid plug at the channel entrance and exit, respectively.

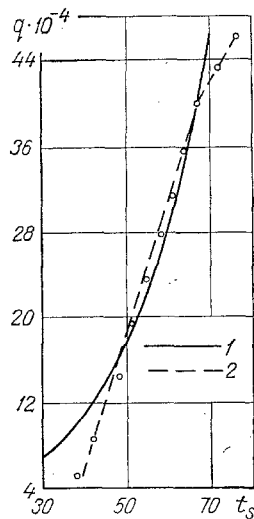


Fig. 3

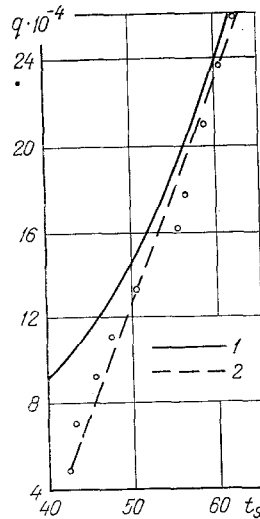


Fig. 4

Fig. 3. Comparison of theoretical and experimental evaluation of a heat pipe: 1) calculation; 2) experiment.

Fig. 4. Comparison of calculations and experimental data for a heat pipe with the evaporator lifted 15 mm above the condenser: 1) calculation; 2) experiment.

When the mass fraction of vapor in the stream is equal to unity at the exit and the heat-transmitting surface is completely irrigated, then the length of the liquid plug at the channel exit tends to its minimum

$$L_{p1} = d \text{ — in cylindrical channels}$$

$$L_{p1} = 2R_{\min} \text{ — in channels of arbitrary shape.}$$

The length of the liquid plug at the channel entrance can be determined from the equation of mass balance

$$(L_{p0} - 2R_{\min}) \rho' = l \rho'', \quad (9)$$

which yields

$$L_{p0} = l \frac{\rho''}{\rho'} + 2R_{\min} \quad (10)$$

Expansion of the vapor plug in a channel is explosive in character. The flow remains laminar within not more than 10% of the total channel length. It therefore is sufficiently accurate to assume a turbulent two-phase stream with

$$\lambda = \frac{0.316}{(N_{Re})^{0.25}} \quad (11)$$

over the entire channel length.

Inserting the values of the referred velocity, the friction coefficient, the length of the liquid plug, and the length of the vapor slug into expression (5), we obtain after integration of the latter

$$\Delta P_f = \frac{0.158}{d_h} \rho' \left( \frac{\mu'}{\rho' d_h} \right)^{0.25} \left( \frac{G_0}{\rho' F} \right)^{1.75} \left( 0.209 l \frac{\rho''}{\rho'} + 0.572 \cdot 2R_{\min} \right). \quad (12)$$

The inertial losses in a homogeneous stream [4] are

$$\frac{dP_i}{dZ} = \left( \frac{G_0}{F} \right)^2 \left\{ \left( \frac{1}{\rho''} - \frac{1}{\rho'} \right) \frac{dx}{dZ} + \frac{dP}{dZ} \left[ x \frac{d}{dP} \left( \frac{1}{\rho''} \right) + (1-x) \frac{d}{dP} \left( \frac{1}{\rho'} \right) \right] - \left[ \frac{1}{\rho'} + x \left( \frac{1}{\rho''} - \frac{1}{\rho'} \right) \right] \frac{1}{F} \frac{dF}{dZ} \right\}. \quad (13)$$

TABLE 1. Calculated and Experimentally Determined Values of the Limiting Thermal Flux

H, mm	t <sub>s</sub> , °C	q <sub>ex</sub> ·10 <sup>-4</sup> , W/m <sup>2</sup>	q <sub>calc</sub> ·10 <sup>-4</sup> , W/m <sup>2</sup>
0	67,5	40,0	41,2
10,5	65	32,5	30,2
13,0	61,5	27,5	26,5
15,0	63,0	25,8	26,3
15,0	56,5	20,7	19,3
17,5	51	14,8	14,7

In the case of circulation of a liquid driven by a capillary pressure head through a channel of uniform cross section, it is permissible to disregard here those terms which account for changes in the density of liquid and vapor due to changes in the pressure, which will reduce expression (13) to

$$\Delta P_1 = \left( \frac{G_0}{F} \right)^2 \left( \frac{1}{\rho'} - \frac{1}{\rho''} \right). \quad (14)$$

When a capillary channel operates in the subcritical range of temperatures, i.e., at temperatures at which the inequality  $\rho'' \ll \rho'$  holds true, then the inertial losses are

$$\Delta P_1 = \rho'' \left( \frac{G_0}{\rho'' F} \right)^2. \quad (15)$$

The magnitude of hydraulic losses  $\Delta P_2$  depends on the mean mass flow rate of the liquid and on the geometry of the wick as well as of the heat pipe. When these parameters are known, then the losses in the wick can be determined from the Darcy equation and the losses in the vapor channel can be determined according to another method [5]. Inserting expressions (1), (3), (12), and (15) into Eq. (2) yields

$$\sigma \left( \frac{1}{R_{\min}} + \frac{1}{R_{\max}} \right) - \Delta P_2 \pm \Delta P_3 = 0.158 \frac{\rho'}{d_h} \left( \frac{\mu'}{\rho' d_h} \right)^{0.25} \left( \frac{Q}{r \rho'' F} \right)^{1.75} \left( 0.209 l \frac{\rho''}{\rho'} + 0.572 \cdot 2 R_{\min} \right) + \rho'' \left( \frac{Q}{r \rho'' F} \right)^2. \quad (16)$$

With the limiting thermal flux in a single capillary channel calculated from expression (16) by the method of successive approximations, we find the thermal flux density in the evaporator which corresponds to the hydrodynamic limit on heat transfer by a heat pipe

$$q = \frac{Q}{F_Q}, \quad (17)$$

where  $F_Q$  is the area of the heat-transmitting surface of a circumferential capillary channel.

The experimental study included checking the performance of a closed capillary structure in the evaporator of a heat pipe and validating the assumption made in the theoretical analysis.

The experimental heat pipe consisted of a tube 14/12 mm in diameter and a hollow sleeve axially fastened to the housing by means of end caps. On the outside surface of this sleeve, within the evaporator zone, were cut a standard M12×1 metric thread along with six 1 mm wide radial through channels as well as six 1-mm-wide and 1-mm-deep axial channels. The sleeve was left smooth, as a plain tube 10/8 mm in diameter, throughout the transport segment and in the condenser. Within the 100-mm-long condenser segment, moreover, the sleeve had 10 through holes 4 mm in diameter each. Both the housing and the sleeve were made of grade 12Kh18N10T steel. The overall length of the pipe was 300 mm, with the evaporator 10 mm long and the condenser 100 mm long.

The performance of this heat pipe was studied with distilled water as the working liquid and with the pipe in a horizontal position as well as in an inclined position opposing the field of body forces. As an example, in Fig. 3 are shown data pertaining to the performance of this heat pipe in a horizontal position. Curve 1 has been calculated according to expressions (16) and (17). A substantial discrepancy between calculations and experiment is evident here in two regions: low and high thermal flux densities. At low thermal flux den-

sities  $q < 17 \cdot 10^4 \text{ W/m}^2$  this discrepancy is due to subcritical operation of capillary channels, with most of the capillary pressure head required for pumping the liquid. At high thermal flux densities  $q > 40 \cdot 10^4 \text{ W/m}^2$  this discrepancy is due to the drying process which now begins. A part of the heat transmitting surface is excluded from useful operation. Only pure vapor flows and the hydraulic losses increase sharply along the segment of a circumferential channel not irrigated by the liquid.

The temperature field around the evaporator periphery was nonuniform. At  $q = 40 \cdot 10^4 \text{ W/m}^2$  and  $t_s = 67.5^\circ\text{C}$ , e.g., the temperature at the outside housing surface was  $t_{\min} = 92.5^\circ\text{C}$  and  $t_{\max} = 126.5^\circ\text{C}$ . However, the average of six temperatures read at six points uniformly spaced around the circumference of one cross section was  $106^\circ\text{C}$ . This nonuniformity of the temperature field was, in these authors' view, caused by some constraints on vapor withdrawal from the lower part of the heat pipe, where apparently a puddle of liquid had formed, and also by the presence of axial feed channels. The theoretical heat-transfer coefficient for axial channels was 3-4 times smaller than that for circumferential channels. As the number of axial channels is decreased and their hydraulic diameter reduced, one should expect the temperature field to become less nonuniform.

Analogous results were obtained with the heat pipe in an inclined position. Performance data characterizing the heat pipe with the evaporator lifted 15 mm above the condenser are shown in Fig. 4; calculated and experimentally determined values of the limiting thermal flux are given in Table 1. These studies of a heat pipe with a closed capillary structure in the evaporator have revealed several valuable features of such a design, the main ones being:

1. Simple Technology. Only the outside surface of the sleeve requires machining. Circumferential, axial, and radial channels can be cut with a standard tool in a conventional lathe.

2. Stable Characteristics. Stability is achieved by convenient manufacturing procedures as well as by accessible and precise inspection of the basic parameters of axial, circumferential, and radial grooves in the sleeve.

3. Vibration and Corrosion Resistance. Vibrations and overloads do not affect the capillary structure, while use of the same material for the housing and for the sleeve precludes corrosive interaction of the two and also broadens the range of structural materials promising for this application.

4. Low Thermal Resistance of the Evaporator. This is achieved by evaporating the liquid from the microfilm surface into the vapor slug. According to available data [4], the film in this design was 30-40  $\mu\text{m}$  thick.

5. High Heat-Transmitting Capacity. Heat pipes with a closed capillary structure excel heat pipes with a reticular wick in performance, within the range of operating temperatures in this study, inasmuch as the limiting thermal flux density in the evaporator is twice as high.

#### NOTATION

$Q$ , thermal flux;  $G$ , mass flow rate;  $r$ , heat of evaporation;  $t_s$ , vapor temperature;  $\sigma$ , coefficient of surface tension;  $R$ , radius of curvature of the interphase boundary;  $Z$ , longitudinal coordinate;  $\lambda$ , friction coefficient;  $J$ , referred velocity of the stream;  $L_p$ , length of the liquid plug;  $L_s$ , length of the vapor slug (bubble);  $l$ , length of the channel;  $x$ , mass fraction of vapor;  $d$ , diameter of the channel;  $F$ , area of an active channel cross section;  $\rho$ , density;  $q$ , thermal flux density;  $\mu$ , dynamic viscosity; and  $H$ , elevation of the evaporator above the condenser; subscripts: "min," minimum; "max," maximum;  $f$ , friction;  $i$ , inertia;  $0$ , channel entrance;  $1$ , channel exit; and  $h$ , hydraulic dimensions; a prime sign, liquid phase; a double prime sign, vapor phase.

#### LITERATURE CITED

1. D. A. Labuntsov, O. P. Evdokimov, I. V. Tishin, and A. F. Ul'yanov, "Analytical study of the boiling process in small-diameter pipes," *Izv. Vyssh. Uchebn. Zaved., Mashinostr.*, No. 7, 61-73 (1970).
2. V. I. Antipov, "Heat transfer during boiling of cryogenic liquids in small-diameter pipes under conditions of forced flow," Candidate's Dissertation, Moscow Institute of Power Engineering, Moscow (1978).

3. V. G. Voronin, A. D. Suslov, V. S. Tarasov, et al., "Heat pipe," Inventor's Certificate No. 544,852 Class F28D15/00, Byull. Izobret., No. 4, 106 (1977).
4. G. Wallis, One-Dimensional Two-Phase Flow, McGraw-Hill (1969).
5. A. Ya. Shelginskii, "Heat and mass transfer in low-temperature heat pipes," Candidate's Dissertation, Moscow Institute of Power Engineering, Moscow (1978).

HEAT AND MASS EXCHANGE WITH VAPORIZATION AND COMBUSTION IN A  
LAMINAR BOUNDARY LAYER OF n-HEXANE AND ETHYL ALCOHOL

G. T. Sergeev, L. I. Tarasevich,  
and G. A. Fateev

UDC 526.536:244.46

Results of an experimental investigation of the combustion of n-hexane and ethyl alcohol in a boundary layer as well as the dependency criteria for calculating the process being examined are presented.

There are only individual works [1-3], many conclusions of which require further refinement, concerning the investigation of heat- and mass-exchange processes under conditions involving combustion of liquid hydrocarbons and alcohols, that have practical and scientific value for chemical technology, physicochemical hydrodynamics, and other areas. Thus, in [1-3], the influence of the transverse flow rate of matter and the depth of the evaporation surface of the injectant, filtered through a porous wall and combusted in an airflow, has not been studied. These problems are examined in the present work.

The combustion of n-hexane and ethyl alcohol was studied experimentally in a low velocity wind tunnel with 0.28×0.34 m rectangular transverse cross section in the working part of the tunnel. The velocity, temperature of the air flow, and the dimensionless parameter of the air blowing in were varied over the following range:  $u_{\infty} = 2-15$  m/sec,  $T_{\infty} = 290-470^{\circ}\text{K}$ ,  $F = (1.24-8.30) \cdot 10^{-3}$  for ethyl alcohol and  $F = (3.39-12.75) \cdot 10^{-3}$  for n-hexane. The local values of the Reynolds numbers varied over the range  $Re_{\Delta x} = 10^3-10^6$ .

The investigation of the combustion of n-hexane and ethyl alcohol was carried out on a porous metallic plate with dimensions 0.196×0.060×0.003 m, separated into four sections. Metallo-ceramic porous plates with a thickness of 0.003 m were pressed out of spherical powder of chrome-plated low-carbon steel with a fraction diameter of 0.063 and 0.1 mm. Their average porosity was about 30%. Copper-constantan thermocouples, whose electrodes had a diameter of 0.1 mm, were affixed to the surface of the porous wall and along its thickness. Each section of the test body was water cooled and was supplied by liquid injectant [1-3]. The temperature in the boundary layer was measured by a Chromel-Alumel thermocouple with a junction diameter of 0.1 mm. The concentrations of the gas components were measured by sampling with the help of a stainless-steel tube with an external diameter of 0.7 mm and a wall thickness of 0.1 mm followed by analysis using a KhL-3 chromatograph. The body was flush mounted to the bottom wall of the working part of the wind tunnel. The experimental setup and the technique used in carrying out the investigations are examined in greater detail in [3].

Typical profiles showing the variation in temperature and concentration along the height of the boundary layer with combustion of n-hexane and ethyl alcohol are shown in Fig. 1. The maximum temperatures  $T_{*}$  in the combustion zone for n-hexane and ethyl alcohol vary in the range 1100-1320 and 1130-1470°K, respectively. The value of  $T_{*}$  is less than the corresponding adiabatic theoretical combustion temperature  $T_{ad}$ , equal to 2397°K for n-hexane and 2350°K for ethyl alcohol. The inequality  $T_{*} < T_{ad}$  stems from losses of heat with exiting gases and chemically incomplete combustion in the maximum temperature zone, occurring with excess air coefficients of  $\alpha = 0.65-0.75$ , as well as some decrease (up to 4%) in the measured temperatures  $T_{*}$  due to convective and radiative heat exchange at the thermocouple junction, respectively,

---

A. V. Lykov Institute of Heat and Mass Transfer, Academy of Sciences of the Belorussian SSR, Minsk. Translated from Inzhenerno-Fizicheskii Zhurnal, Vol. 40, No. 4, pp. 604-607, April, 1981. Original article submitted February 29, 1980.